An actin-dependent conformational change in myosin

Ming Xiao[1,2], Jeff G. Reifenberger[1], Amber L. Wells[3], Corry Baldacchino[3], Li-Qiong Chen[3], Pinghua Ge[1], H. Lee Sweeney[3] and Paul R. Selvin[1,4]

Published online 7 April 2003; doi:10.1038/nsb916

Conformational changes within myosin lead to its movement relative to an actin filament. Several crystal structures exist for myosin bound to various nucleotides, but none with bound actin. Therefore, the effect of actin on the structure of myosin is poorly understood. Here we show that the swing of smooth muscle myosin lever arm requires both ADP and actin. This is the first direct observation that a conformation of myosin is dependent on actin. Conformational changes within myosin were monitored using fluorescence resonance energy transfer techniques. A cysteine-reactive probe is site-specifically labeled on a 'cysteine-light' myosin variant, in which the native reactive cysteines were removed and a cysteine engineered at a desired position. Using this construct, we show that the actin-dependent ADP swing causes an 18 Å change in distance between a probe on the 25/50 kDa loop on the catalytic domain and a probe on the regulatory light chain, corresponding to a 23° swing of the light-chain domain.

Nucleotide-induced conformational changes within myosin cause a relative movement of myosin with respect to actin, thereby converting the chemical energy in ATP into mechanical work[1–3]. However, how, or if, these nucleotide-induced changes are dependent on the presence of actin is unclear. Answering this question is critical for several reasons. First, if there are actin-dependent conformational changes, then the current crystal structures, all without actin, may not cover the entire set of actual conformational changes that occur during the catalytic cycle. Second, the critical step in the catalytic cycle that leads to myosin movement, the 'powerstroke', inherently occurs in the presence of actin, but the 'swinging lever arm' model to explain this powerstroke is largely based upon crystal structures that lack actin. Third, actin-induced conformational changes are central to myosin activity — for example, the ATPase activity of myosin increases >100-fold upon actin binding. However, these changes have not yet been detected through structural analysis, although an ADP-dissociation–induced closure of the cleft within the actin-bound myosin head has been suggested from electron microscopic data[4].

The available myosin crystal structures, as well as spectroscopic studies of the myosin head, indicate that the myosin powerstroke arises from a rotation of the light chain domain of myosin relative to the catalytic domain when myosin undergoes a transition from an ADP-P_i state to an ADP state. However, most myosins — including smooth and cardiac muscle myosin

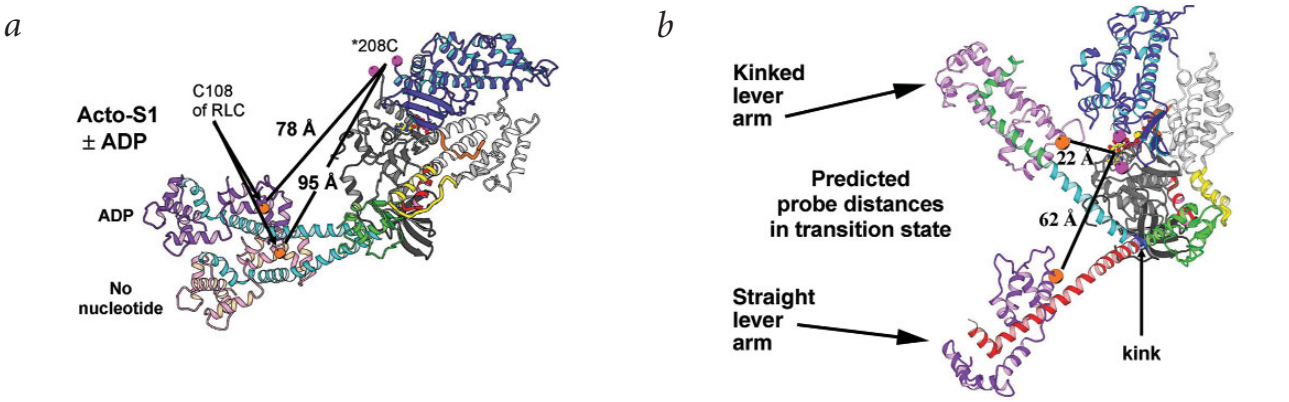

Fig. 1 Position of probes and predicted Cα distances from cryo-EM docking of crystal structures for acto-S1 (S1 = single-headed subfragment 1 of myosin) ± ADP and transition state (S1–vanadate) with and without a 'kink' in lever arm. Orange represents a probe on the regulatory light chain at position Cys108. Pink represents the two residues that are found in the crystal structure surrounding S208C. The other FRET/LRET probe is placed on S208C, which is in a disordered loop in the crystal structure. The distances shown are the distance between Cα of Cys108 and the average position of Val104 (amino acid corresponding to Cys108 in the smooth RLC) and residues flanking S208C. ***a***, Nucleotide-free structure of myosin S1 fragment and the same structure with light chain domain rotated about Gly770 (labeled as 'ADP') for docking into the myosin–ADP–actin electron microscopy image of Whittaker *et al.*[5] Comparing S1–actin to S1–actin–ADP, the predicted distance change from the cryo-EM data is 17 Å. using LRET we find a change of 19.5 ± 4.5 Å and from FRET we find a change of 17.0 Å. ***b***, Crystal structure of Dominguez *et al.*[2] showing a 22 Å distance between probes, and the same crystal structure except without the 'kink' in the lever arm, which predicts a 62 Å distance between the probes.

[1]Department of Physics, University of Illinois, 1110 West Green Street, Urbana, Illinois 61801, USA. [2]Current address: Cardiovascular Research Institute, University of California, San Francisco, California 94143, USA. [3]Department of Physiology, University of Pennsylvania School of Medicine, 3700 Hamilton Walk, Philadelphia, Pennsylvania 19104-6085, USA. [4]Center for Biophysics and Computational Biology, University of Illinois, Urbana, Illinois 61801, USA.

Correspondence should be addressed to P.R.S. *e-mail: selvin@uiuc.edu* or H.L.S. *e-mail: lsweeney@mail.med.upenn.edu*

Table 1 Activity of cys-light smooth S1 myosin *versus* wild type[1]

	Smooth wild type S1	Cys-light S1[2]
K^+-EDTA ATPase	2.2 ± 0.4	1.8 ± 0.5 (82)
Actin-activated V_{max}	1.1 ± 0.3	0.9 ± 0.2 (82)
ADP–actomyosin dissociation rate	78 ± 4	74 ± 0.5 (95)

[1]In unit of sec^{-1}.
[2]Number in parentheses is the percent activity of wild type.

II, all non-muscle myosin IIs, myosin V, myosin VI and brush border myosin I — also display an additional rotation of the light chain domain upon release of ADP when bound to actin[5,6]. For smooth muscle myosin, this additional rotation may be necessary before ADP can be released, thereby slowing the release of ADP. Physiologically, this may be associated with the 'latch' state — that is, the ability of smooth muscle to generate high tension with minimal ATP turnover.

Here we report the first direct measurement of an actin-dependent conformational change in myosin. Specifically, we show that the lever arm swing upon ADP release in smooth muscle myosin occurs only when actin is present. Fluorescence resonance energy transfer (FRET) techniques that are sensitive to the relatively long distances involved (60–90 Å between probes) in the conformations are used in this study. To simplify the system, we generated a mutant smooth muscle myosin in which all unwanted reactive cysteines have been removed and a cysteine has been introduced for site-specific probe placement. FRET relies on the distant-dependent transfer of energy from an excited donor dye to an acceptor dye (see Methods). A modification of this technique, lanthanide resonance energy transfer (LRET), uses a luminescent lanthanide atom as the donor, which transfers energy in a similarly distant-dependent fashion[7].

Activity of Cys-light myosin

We created a construct in which nine cysteines on the heavy chain and three cysteines on the essential light chain (ELC) were removed from the native smooth S1 myosin head. An additional cysteine at position 208 of the heavy chain was inserted, and the native cysteine at position 108 of the regulatory light chain (RLC) was left intact (this construct is termed Cys-light S1 or Cys-light myosin). The actin-activated and K^+-EDTA ATPase activity, as well as the ADP dissociation rate from actomyosin of the Cys-light myosin indicate that the Cys-light myosin has near wild type activity (Table 1). We do find, however, that the Cys-light myosin is significantly more unstable than wild type and requires the presence of nucleotide or actin to be stable for periods longer than ~30 min. Even under these conditions, a fraction of heads generally appears to be stuck in a rigor-like conformation ('dead heads') (see below).

Probe type, position and labeling specificity

The FRET or LRET probes were placed on position 108 of the RLC and position 208 in the 25/50 kDa loop of the heavy chain. To estimate the magnitude of the conformational change in myosin, we measured the distances of the labeling sites in the nucleotide-free myosin S1 crystal structure (assumed to be in the rigor state)[1,8] (Fig. 1*a*, no nucleotide) and in the same structure docked into the myosin–ADP–actin electron microscopy image of Whittaker *et al.*[5], where the light chain domain is rotated (Fig. 1*a*, ADP) by 23°. It is difficult to accurately determine the distance between the probes because residue 208 is in a disordered loop in the crystal structure. Nevertheless, as a rough guide, the distance between Cys108 on the RLC and the average position of two residues seen in the crystal structure surrounding amino acid 208 is 95 Å with no nucleotide and 78 Å with ADP bound. Hence, a change of 17 Å is predicted by the cryo-EM data with or without ADP in the presence of actin.

There are two possible conformations of myosin in complex with Mg–ADP–BeF_3, a transition-state (ADP-Pi) analog (Fig. 1*b*). Based on the crystal structure of smooth muscle myosin[2], which has a large kink in the lever arm, a distance of 22 Å between the probes is predicted. If this kink is absent, at least in a subpopulation, as suggested by the FRET studies of Shih *et al.*[9], the predicted distance is 62 Å.

LRET intensity measurements

Energy transfer efficiencies and distances can be measured by comparing donor and acceptor emission intensities when the quantum yields of the dyes are known (see Methods). The curve of the time-delayed spectra of donor-only-S1 has the usual highly spiked shape of the terbium emission spectrum (Fig. 2; Table 2). The donor-only spectrum is independent of nucleotide and actin. The donor-S1-acceptor (D-A) samples have a pronounced rise in emission beyond 560 nm (Fig. 2), which is due solely to emission of the acceptor dye after receiving energy from the donor; the time-delay completely eliminates any fluorescence of the acceptor due to direct excitation. Because the acceptor and Tb^{3+} donor quantum yields are independent of bound ligands (data not shown), a change in the sensitized emission can be directly interpreted as a change in the energy transfer between the probes (see Methods). Using measured quantum yields of donors and acceptors (see Methods) we calculated energy transfer efficiencies and distances between the probes in a variety of conditions (Table 2). These values were corrected, when appropriate, for a fraction of dead S1 heads that appear not to bind nucleotide (see Methods).

On the basis of the relative areas under the spectra, the distances for the sample in the absence of nucleotide (red), with

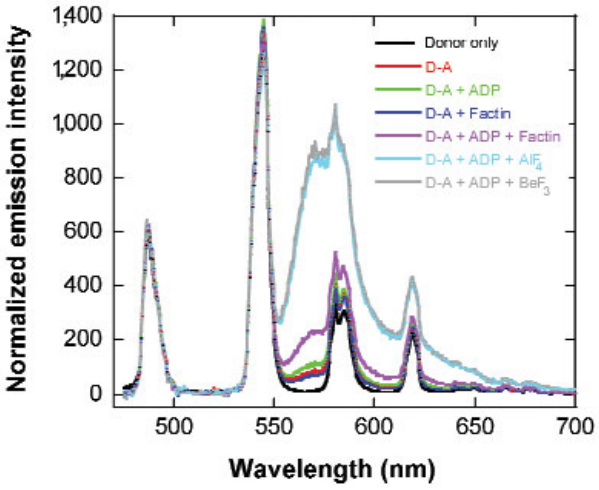

Fig. 2 Time-delayed LRET spectrum of myosin as a function of nucleotide and actin binding. All data were collected after a 26 μs delay to eliminate fluorescence from the acceptor due to direct excitation. Data are normalized to donor peak at 490 nm. Terbium displays the characteristic sharply spiked spectra with peaks at 490, 546, 585 and 620 nm (donor only, black). The broad emission around 560 nm is sensitized emission of acceptor resulting from energy transfer from the donor.

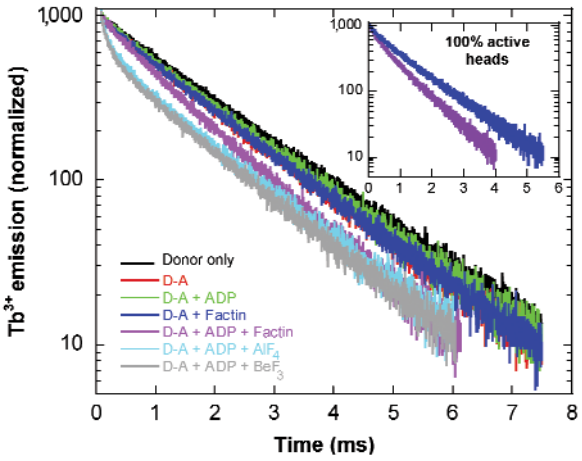

Fig. 3 Terbium lifetime (using fluorescence at 546 nm) as a function of bound ligand. Terbium lifetimes can be used to infer energy transfer efficiencies and interprobe distances and, hence, conformational changes in myosin. Lifetime curves correspond to the myosin preparation whose spectrum is shown in Fig. 2 and confirm the spectral measurements. They also reveal that in this myosin preparation ~70% of myosin is trapped with AlF_4 or BeF_3, with the remaining 30% stuck in a rigor-like (D-A) conformation. A second preparation yielded 100% active heads (inset).

ADP (green) or with actin (blue) are similar and average 77.4 Å (Fig. 2). This compares with the rough estimate of 95 Å in the cryo-EM reconstruction (see above). Adding both ADP and actin to the donor-S1-acceptor samples led to significantly increased sensitized emission (magenta curve), corresponding to an average energy transfer of 31% and a distance of 60.5 Å. Hence, the distance between the probes is shortened by 16.9 Å (relative to the myosin in the absence of nucleotide and actin) in the presence of both ADP and F-actin but not with ADP alone or actin alone. This is in agreement with the change of 17 Å predicted by cryo-EM but now shows that the change is actin dependent. The small changes in distance seen with ADP-only or F-actin–only, compared with S1 without nucleotide or actin, are probably not statistically significant because they were irreproducible upon repeat measurements on a different sample or lifetime measurements on the same sample. Simulating a transition state in the myosin cycle by trapping the myosin in the absence of actin with the phosphate analogs Mg–ADP–AlF_4 (light blue) or Mg–ADP–BeF_3 (gray) leads to yet larger sensitized emission (Fig. 2). This corresponds to an average distance of 45 Å or a shortening of 33 Å between the probes, compared with the nucleotide-free (rigor) state. This is significantly longer than the 22 Å distance predicted by the crystal structure of smooth muscle myosin trapped with Mg–ADP–AlF_4 or Mg–ADP–BeF_3 and between the 22–62 Å distances predicted by the FRET measurements of Shih *et al.*[9]

LRET donor lifetime measurements

The changes in the donor emission lifetime (Fig. 3) can be used to calculate energy transfer and distances (see Methods; Table 2). The terbium signal from donor-only-S1 is nearly single exponential, with 90% having a lifetime of 1.74 ms and 10% having a lifetime of 0.67 ms. We used the average lifetime, 1.64 ms, to calculate energy transfer efficiencies. The terbium lifetime decreases in the presence of acceptor (D-A), yielding 11% energy transfer for no nucleotide and a distance of 78 Å, in excellent agreement with 77.4 Å average distance derived from intensity measurements described above. No significant changes are seen upon addition of either ADP or F-actin alone. However, addition of both ADP and F-actin significantly decreases the average lifetime. Two populations of terbium-labeled S1 can be resolved: 69% of the S1 fit to an average lifetime 1.02 ms, corresponding to 38% energy transfer and a 60 Å distance, and 31% of the S1 fit to the 1.46 ms no-nucleotide D-A lifetime. We interpret the 31% population as dead heads that are stuck in a rigor-like conformation and undergo no conformational change. The remaining

Table 2 Energy transfer efficiencies, distances and distance changes between probes on S208C in the catalytic domain and C108 of RLC of Cys-light S1

S1 Myosin	No ligand	ADP	F-actin	ADP + F-actin	ADP–AlF_4	ADP–BeF_3
LRET intensity (spectrum)[1]						
ET (%)	11 (8)	14	9 (9)	33 (29)	85 (61)	81(62)
Distance (Å)	79 (77)	75	81 (75)	62 (59)	41 (48)	44 (47)
ΔDistance (Å)[2]	NA	–4.0	2.7 (–2.0)	–17 (–18)	–38 (–30)	–35 (–30)
LRET donor lifetime[1]						
ET (%)	11	9	12 (6)	38 (37)	82 (72)	83 (65)
Distance (Å)	78	81	77 (82)	60 (56)	43 (44)	42 (46)
ΔDistance (Å)[2]	NA	3	–1 (4)	–18 (–22)	–35 (–34)	–36 (–32)
LRET sensitized emission						
ET (%)[3]	–	–	–	45–60[4]	70	71
Distance (Å)[2]	–	–	–	51–57[4]	48	47
FRET[5]						
ET (%)	8.4	9.6	9.7	22	41	35
Distance (Å)	100	98	97	83	71	76
ΔDistance (Å)[2]	NA	–2.5	–2.6	–17	–29	–24

[1]The values not in parentheses (in parentheses) represent two different protein preparations.
[2]Distance changes are relative to the no-ligand case. 'NA' is 'not applicable'.
[3]For No ligand, ADP and F-actin, robust distances could not be extracted from the curve-fits.
[4]The distance range reported was fairly sensitive to curve-fitting assumptions. The range of values represents the extreme values for different curve-fitting assumptions (see Methods).
[5]FRET data were taken on the same sample as the LRET data, which showed 31% dead heads. FRET values are corrected for the fraction of dead heads. FRET measurements on a separate protein preparation yielded similar results — an ADP swing only in the presence of actin (S1–ADP ± actin of 21.8 Å assuming 100% active heads and complete labeling). The fraction of dead heads for the second repeat measurement was not determined.

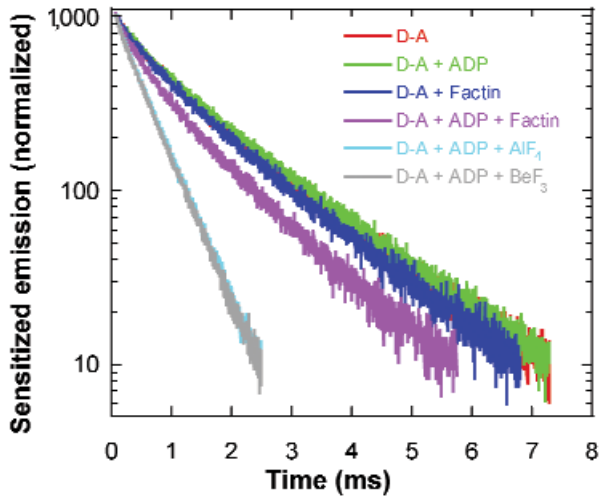

Fig. 4 Sensitized emission lifetime (measured at 570 nm) as a function of bound ligand. Shorter lifetime indicates more energy transfer and shorter interprobe distances. Data shown is for the same myosin preparation shown in Figs. 2, 3.

69% of the S1 are active and undergo an 18 Å shortening compared with the rigor condition. (Other samples that were left without nucleotide for an extended period of time and showed no conformational changes and displayed energy transfer efficiencies characteristic of the rigor state.) A repeat on a second sample (Table 2; inset of Fig. 3) in which all the heads are active yielded a 22 Å shortening upon addition of ADP and actin. These values are consistent with the 17 Å distance changes inferred from the intensity spectra (Fig. 2; Table 2). This repeat measurement on a fully active sample also confirms our interpretation that the 31% population seen in the first sample is due to inactive heads and not some active, altered conformation. Adding either Mg–ADP–AlF_4 or Mg–ADP–BeF_3 to S1 leads to a further shortening of the donor lifetime; a bi-exponential decay can clearly be seen. One population (amplitude of 38% with AlF_4 sample; 32% with BeF_3 sample) has the rigor-like lifetime, which we interpret as myosin heads that did not get trapped, likely because they are inactive. For ADP–AlF_4 (ADP–BeF_3), the remaining 62% (68%) of the population has 0.31 (0.27) ms lifetime, corresponding to 81% (83%) energy transfer and a distance of 43 Å (42 Å). This distance is in excellent agreement with the intensity measurements. Hence, trapping the S1 with either of these phosphate analogs lead to a shortening of the donor–acceptor distance by ~35 Å compared with the no-nucleotide condition. The fraction of dead heads estimated by the ADP plus F-actin condition (31%) and by the ADP–AlF_4 (38%) and BeF_3 sample (32%) are also in good agreement with each other. In addition, the absolute distances of 42–43 Å, although significantly shorter than the rigor condition, are also much larger than the 22 Å expected based on the crystal structure of Dominguez *et al.*[2] (see below).

LRET sensitized emission lifetime measurements

We also measured energy transfer using changes in sensitized emission lifetimes (Fig. 4; Table 2). The trend in the sensitized emission lifetimes (Fig. 4) follows the trend shown in the donor lifetime and intensity measurements. The acceptor in S1 without nucleotide, ADP or F-actin displays a relatively long sensitized emission lifetime, corresponding to a small amount of energy transfer. Upon addition of both ADP and F-actin, the lifetime decreases and, hence, energy transfer significantly increases. S1 bound to Mg–ADP–AlF_4 or Mg–ADP–BeF_3 displays even greater energy transfer. Robust curve fits and distances were not possible for the rigor, ADP and F-actin cases (see Methods). Curve fits for the ADP plus F-actin condition yielded distances ranging from 51–57 Å, depending on whether or not a fraction of dead heads was assumed. This is in good agreement with the 56–62 Å range of distances found *via* donor lifetime and intensity measurements. Robust curve fits for the ADP–AlF_4 or ADP–BeF_3 yielded distances of 47–48 Å, which were also in good agreement with the donor lifetime and intensity measurements.

FRET measurements

The LRET measurements were further confirmed *via* steady-state FRET measurements. In general, FRET measurements are more sensitive to the angular orientation of the dyes and therefore are less reliable in terms of absolute distances, although they provide a general consistency check for the LRET results. We determined the steady-state FRET spectra in which the direct acceptor emission had been removed, and all signals were normalized to the Alexa 546 donor peak around 580 nm (Fig. 5). Using Eq. 1 and Eq. 2 (see Methods) and the measured quantum yields of Alexa 546 on C108 (0.58) and Cy5 on S208C (0.51), distances were determined. Consistent with the LRET results, addition of ADP or F-actin to the myosin does not lead to changes in energy transfer, but addition of both ADP and F-actin together causes a significant (17 Å) shortening of distances. Trapping the myosin with ADP–AlF_4 or ADP–BeF_3 lead to yet further shortening that is, yet again, significantly longer than that expected from the crystal structure of smooth muscle myosin trapped with these nucleotide analogs[2] (see below). Lifetime FRET measurements (data not shown) further confirm this trend; however, multi-exponential donor-only lifetimes made a detailed quantitative comparison difficult. Because steady-state FRET measurements detect average properties and are not able to detect heterogeneity within a sample, we assumed the fraction of

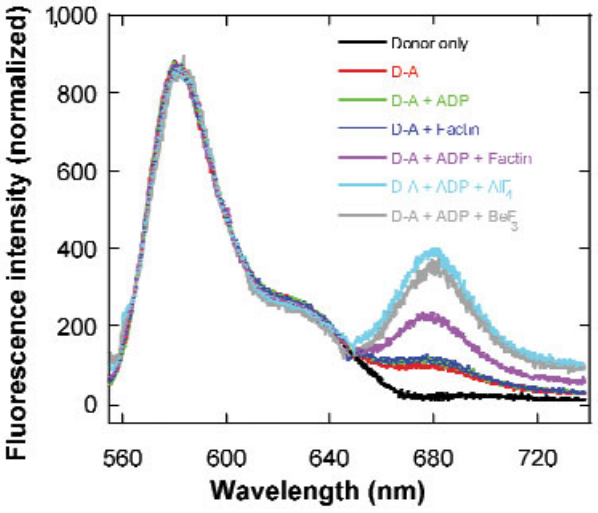

Fig. 5 Steady-state FRET data. The Alexa 546 donor emits maximally at ~580 nm; and the Cy5 acceptor, ~680 nm. Direct excitation of the acceptor has been subtracted from the spectrum (see Methods). An increase in acceptor (sensitized emission) fluorescence indicates greater energy transfer and shorter interprobe distances. An increase in energy transfer is clearly seen upon addition of both ADP and F-actin, but not with ADP alone or F-actin alone. Additional energy transfer is seen when the myosin is trapped with phosphate analogs ADP–AlF_4 or ADP–BeF_3.

dead heads was the same as measured *via* lifetime LRET when using the same protein preparation. However, our conclusion that the ADP swing of myosin is dependent on actin is independent of this assumption.

The absolute distances measured *via* FRET are in reasonable agreement with the distances predicted by cryo-EM: 100 Å *versus* 95 Å in rigor-like states (S1–ADP, S1–actin and nucleotide-free S1) and 83 Å *versus* 78 Å in the S1–ADP–F-actin state for the FRET and cryo-EM distances, respectively (Fig. 1*a*). These are significantly larger than the distances found *via* LRET (78.3 ± 2.6 Å and 59.2 ± 2.5 Å, respectively). This difference could be due to a number of factors: a different position of the FRET *versus* LRET probe when attached to S208C; a different position of the disordered loop containing residue 208 when the different probes are bound; a fraction of Cy5 acceptor molecules that are non-absorbing; uncertainties in R_o, particularly for FRET; and protein dynamics during the ms lifetime of the terbium donor, which can bring the probes closer together during LRET. However, changes in distance — such as the actin-dependent ADP swing — are less sensitive to these effects. Indeed, comparing the nucleotide-free S1 to S1–ADP–F-actin, FRET yields a distance change of 17 Å and LRET yields a change of 18.8 Å.

Discussion

Does the ADP swing of smooth muscle myosin depend on actin? The major finding of this study is that the ADP swing of smooth muscle myosin is actin dependent. Combining all the energy transfer measurements, addition of ADP or F-actin to nucleotide-free S1 leads to no significant changes in donor–acceptor distance (–1.2 ± 3.6 Å and +0.2 ± 2.95 Å, respectively). In contrast, addition of both ADP and F-actin to S1 leads to a shortening of the distance between probes of 18.4 ± 2.1 Å. Similarly, comparing S1–actin to S1–actin–ADP leads to a change in distance of 18.4 ± 4.6 Å, which is in excellent agreement with the 17 Å change predicted by the cryo-EM on decorated filaments[5]. The most straightforward model to account for these changes is a rigid-body rotation of the light chain domain by 23° upon ADP release in the presence of actin. However, the motion may be more complex, involving a twisting of the light chain domain as well[4].

We can now conclude that (i) the ADP–S1–actin conformation is unique to the actin-bound state and is not significantly populated in the absence of actin; (ii) in the absence of actin, the ADP and no nucleotide states of smooth muscle myosin S1 are similar in terms of lever arm position, and this position is similar to the rigor conformation (where rigor is defined as the S1–actin-no-nucleotide state); and (iii) the lever arm position is rigor-like in all crystal forms other than the pre-powerstroke state. Thus, the actin–myosin–ADP state of smooth muscle myosin II, and likely of many other myosin family members, may be achieved only when the motor domain is bound strongly to actin and ADP is tightly bound at the active site.

Is there a kink in the light-chain domain in the transition state? Crystal structures of smooth muscle myosin in the pre-powerstroke state, with either BeF_3 or AlF_4 phosphate analogs trapped at the active site, show a pronounced kink in the light chain helix at the point where it emerges from the converter domain of the motor[2] (Fig. 1*b*). This has been suggested to indicate a flexible point in the light-chain domain[10,11]. Whether the kink is due to crystal packing forces and/or is present in solution is unclear. A solution-based FRET study[9] detected two conformations of *Dictyostelium* myosin S1 with the phosphate-analog vanadate trapped in the active site. One conformation is consistent with a kink in the light chain domain; and the second, with an undistorted light chain helix, has been seen for scallop S1 (refs. 10,11). The two structures, if present in our measurements, would yield interprobe distances of ~22 Å and 62 Å. Our FRET result yields 73.5 Å, consistent with a myosin structure without a kink. Our LRET results yield 45 ± 2.5 Å, which is more difficult to interpret, although arguably more consistent with an undistorted light chain. The reason for this is that the energy transfer efficiency and, therefore, the distance derived from a LRET measurement are heavily weighted toward the distance of closest approach if dynamics are present during the ms donor lifetime. Hence, a straight lever arm that had flexibility could yield a distance of 45 Å, even if the average distance was closer to 62 Å. In contrast, dynamics would not make a 22 Å average distance appear to be the larger value of 45 Å.

One interpretation consistent with all three studies is that the kink represents a flexible point, and the population of bent and straight lever arms depends on experimental conditions. Crystal packing forces and light-chain–heavy-chain interactions seen in the crystal structure, and possibly present in solution, stabilize the bent form. However, in solution and without crystal packing forces, an equilibrium exists between the two forms, as seen by Shih *et al.*[9]. In our study, probes in the 25/50 kDa loop likely prevent the light-chain–heavy-chain interactions and, therefore, may shift the solution equilibrium to a straight form. There are, however, several subtle differences between the studies: Shih *et al.*[9] used *Dictyostelium* myosin with vanadate as a phosphate analog, whereas we and Dominguez *et al.*[2] have used smooth muscle myosin with AlF_4 and BeF_3 analogs. Hence, a definitive conclusion about the lever arm kink in smooth muscle myosin must await future experiments in which probes are placed at alternative positions on the heavy chain and vanadate is used as a phosphate analog.

Methods

Construction of Cys-free smooth S1. The cDNA for chicken gizzard smooth muscle myosin was truncated at the codon corresponding to amino acid 859 to create an S1-like fragment. To allow for affinity purification, a FLAG peptide sequence[12] was appended, followed by a stop codon. Site-directed mutagenesis was used to remove all reactive cysteines in the heavy chain (C94H/C121L/C481V/C524T/C545S/C582S/C707T/C717T/ C829S). A single reactive cysteine (S208C) was then inserted in the 25/50 kDa loop (loop 1) of the heavy chain in the catalytic domain for labeling with dyes (Fig. 1). Reactive cysteines were also removed from the essential light chain (C2S/C85T/C138N). The wild type RLC contains one cysteine (Cys108), which was left intact to serve as a labeling site. The mutant S1 and light chains were subcloned into the baculovirus transfer vector, pVL1393 (Invitrogen). Generation of the recombinant baculoviruses coding for the S1 and light chain constructs followed published procedures[13].

Expression and purification of proteins. Baculovirus expression was used to produce S1-like fragments of the cysteine-light chicken smooth muscle myosin II. This involved infection of an insect cell line (SF9) with a recombinant baculovirus that is able to drive high level expression of foreign protein under the polyhedron promoter. SF9 cells were co-infected with recombinant virus containing the cysteine-deficient ELC (LC_{17a}) cDNA and with recombinant virus encoding a truncated myosin heavy chain. Purification and assays of actin/myosin ATPase activity followed published procedures[14]. The sole exception was that the isolated myosin was devoid of RLC because RLC-encoding virus was not used. Thus, labeled (see below) RLC was added during the purification (following release from actin and before addition to an anti-FLAG–affinity column). Steady-state MgATPase rates (25 °C with [γ-^{32}P]ATP) and K^+-EDTA ATPase activity

were measured by the methods of Pollard[15], and the ADP dissociation rate was measured according to White[16].

Labeling and trapping of biochemical states. The myosin heavy chain at S208C was labeled with Tb–DTPA–cs124–MEA or Tb–DTPA–cs124–EMPH[17] as the LRET donor, or Cy5 (Amersham) as the FRET acceptor. The terbium chelates are similar in size to conventional fluorescent probes[18]. The RLC was labeled with 5-tetramethylrhodamine maleimide as the acceptor for the Tb–DTPA–cs124–MEA (Table 2, LRET numbers in parenthesis) or Alexa 546 C_5 maleimide (Molecular Probes) as the acceptor for Tb–DTPA–cs124–EMPH (Table 2, LRET numbers not in parentheses). The labeled RLC was exchanged into the heavy chain and purified by fast performance liquid chromatography. For FRET measurements, two organic dyes were used as fluorescent probes: Alexa 546 was the donor placed on the RLC, and Cy5 was the acceptor placed on the heavy chain. For FRET and LRET labeling, we tested the specificity of labeling *via* a negative control; we used a cys-light S1 with a native residue at position 208 and a cysteine-free RLC, and found no detectable labeling (data not shown). Myosin was trapped with BeF_3 or AlF_4 according to standard methods[19]. Proteins were diluted to ~1 μM for spectroscopy.

FRET and LRET spectroscopy. For LRET, the instrumentation and methodology has been described[20]. Briefly, samples were excited with a 5 ns pulse at 337 nm. Luminescence from the terbium donor (at 490 or 546 nm) or from the sensitized emission of the acceptor (at 570 nm) was then collected as a function of time with 2 μs resolution. Pulses were repeated 40× per s, and the resulting signals were averaged to yield the donor or sensitized-emission excited-state lifetimes. Lifetimes were fit to multi-exponential decays. The minimum number of exponentials consistent with no residual structure was used.

For steady-state FRET measurements, the donor was excited at 543 nm with a He-Ne laser, and the emission spectra of the donor–acceptor was recorded at all wavelengths simultaneously[20]. To calculate the energy transfer efficiency from the FRET emission spectra, the direct acceptor fluorescence was subtracted from the donor/acceptor spectrum (Eq. 2). This was accomplished by excitation at 633 nm, where only the acceptor absorbs, and multiplying this intensity by the ratio of fluorescence of an acceptor-only sample excited at 540 nm and 640 nm[21].

FRET and LRET energy transfer and distance determination. Distances (R) between the donor and acceptor were determined *via* the conventional Forster equation:

$$R = R_o\,(1 / E - 1)^{1/6} \qquad (1)$$

where R_o is calculated from the spectral properties of dyes, assuming the dyes rapidly reorient during their excited state lifetimes (see below). E is determined by measuring the intensity of the sensitized emission (I_{ad}) and comparing it to the residual donor emission in the presence of acceptor (I_{da}), normalized by their quantum yields (Eq. 2) or by measuring the excited-state lifetimes (Eq. 3):

$$E = (I_{ad} / Q_a) / (I_{da} / Q_d + I_{ad} / Q_a) \qquad (2)$$

$$E = 1 - (\tau_{da} / \tau_d) = 1 - (\tau_{ad} / \tau_d) \qquad (3)$$

where τ_{da} and τ_d are the excited-state lifetime (intensity) of the donor in the presence and absence of the acceptor, respectively, and τ_{ad} is the lifetime of the sensitized emission. Q_a is the quantum yield of the acceptor, and Q_d is quantum yield for the donor in the absence of acceptor.

Lifetime measurements, but not intensity measurements, are able to identify heterogeneity in a population. As mentioned, a fraction of heads was sometime stuck in a rigor-like conformation, as determined by LRET lifetime measurements. The relative population could be determined from the fractional amplitudes of the lifetime decays. This fraction was then used to correct the intensity (spectral) measurements of the non-rigor like states — that is, the ADP–F-actin, ADP–BeF_3, and ADP–AlF_4 states — to yield a corrected energy transfer efficiency. R was calculated from this E.

Quantum yield, anisotropy and R_o values of dyes. The quantum yields of Alexa 546 maleimide (0.58)or tetramethylrhodamine (Molecular Probes) maleimide (0.45) (bound to RLC and exchanged into S1, or Cy5 at position S208C of the heavy chain) were measured by a steady-state intensity comparison to free tetramethylrhodamine standard of quantum yield of 0.52 (ref. 22) or free Cy5 (quantum yield = 0.4)[23]. The quantum yield of TMRM bound to RLC (quantum yield. = 0.45) was previously determined[19]. The quantum yields of Tb–DTPA–cs124–MEA (<τ> = 1.06 m; quantum yield = 0.33) and Tb–DTPA–cs124–EMPH (<τ> = 1.64 ms; quantum yield = 0.51) were measured by lifetime comparison to free Tb–DTPA–cs124 (τ = 1.55 ms; quantum yield = 0.48)[23]. The emission polarization of Tb^{3+} in DTPA–cs124 chelates had been shown to be unpolarized[23]. The emission anisotropy of Alexa 546 and TMRM bound to RLC was measured *via* standard techniques and found to be 0.29 and 0.28, respectively[19]. The emission anisotropy of Cy5 on S208C was found to be 0.19.

The R_o values for various donor/acceptor pairs were calculated *via* standard techniques using the appropriate quantum yields and assuming rapid reorientation of dyes: κ^2 (orientation factor) = 2/3 (ref. 24). For LRET using Tb–DTPA–cs124–MEA to TMR, R_o = 51.3 Å; and for Tb–DTPA–cs124–EMPH to Alexa 546 Flour, R_o = 55.2 Å. For FRET using Alexa 546 to Cy5, R_o = 67 Å. For FRET, because of the finite polarization of the donor and acceptor, $0.15 < \kappa^2 < 2.87$ and $52.5\ Å < R_o < 85.6\ Å$. This leads to a maximum error in R of +28% and –22% if one sets $\kappa^2 = 2/3$. For LRET, because of the finite polarization of the acceptor, $0.43 < \kappa^2 < 1.13$, which leads to a maximum error in R of +9% / –7% if one sets $\kappa^2 = 2/3$.

Acknowledgments
This work was supported by NIH grants to P.R.S. and H.L.S.

Competing interests statement
The authors declare that they have no competing financial interests.

Received 12 October, 2002; accepted 5 March, 2003.

1. Rayment, I. *et al*. Structure of the actin–myosin complex and its implications for muscle contraction. *Science* **261**, 58–65 (1993).
2. Dominguez, R., Freyzon, Y., Trybus, K.M. & Cohen, C. Crystal structure of a vertebrate smooth muscle myosin motor domain and its complex with the essential light chain: visualization of the pre-power stroke state. *Cell* **94**, 559–571 (1998).
3. Houdusse, A., Kalabokis, V.N., Himmel, D., Szent-Györgyi, A.G. & Cohen, C. Atomic structure of scallop myosin subfragment S1 complexed with MgADP: a novel formation of the myosin head. *Cell* **97**, 459–470 (1999).
4. Volkmann, N. *et al*. Evidence for cleft closure in actomyosin upon ADP release. *Nat. Struct. Biol.* **7**, 1147–1155 (2000).
5. Whittaker, M. *et al*. A 35 Å movement of smooth muscle myosin on ADP release. *Nature* **378**, 748–751 (1995).
6. Gollub, J., Cremo, C.R. & Cooke, R. ADP release produces a rotation of the neck region of smooth myosin but not skeletal myosin. *Nat. Struct. Biol.* **3**, 796–802 (1996).
7. Selvin, P.R. Principles and biophysical applications of luminescent lanthanide probes. *Annu. Rev. Biophys. Biomol. Struct.* **31**, 275–302 (2002).
8. Rayment, I. *et al*. Three-dimensional structure of myosin subfragment-1: a molecular motor. *Science* **261**, 50–57 (1993).
9. Shih, W.M., Gryczynski, Z., Lakowicz, J.R. & Spudich, J.A. A FRET-based sensor reveals large ATP hydrolysis-induced conformational changes and three distinct states of the molecular motor myosin. *Cell* **102**, 683–694 (2000).
10. Houdusse, A., Szent-Gyorgyi, A.G. & Cohen, C. Three conformational states of scallop myosin S1. *Proc. Natl. Acad. Sci. USA* **97**, 11238–11243 (2000).
11. Houdusse, A. & Sweeney, H.L. Myosin motors: missing structures and hidden springs. *Curr. Opin. Struct. Biol.* **11**, 182–194 (2001).
12. Hopp, T.P. *et al*. A short polypeptide marker sequence usefulfor recombinant protein identification and purification. *Biotechnology* **6**, 1205-1210 (1988).
13. O'Reilly, D.R., Miller, L.K. & Luckow, V.A. *Baculovirus Expression Vectors: a laboratory manual* (W.H. Freeman and Company, New York, New York; 1992).
14. Sweeney, H.L. *et al*. Kinetic tuning of myosin *via* a flexible loop adjacent to the nucleotide binding pocket. *J. Biol. Chem.* **273**, 6262–6270 (1998).
15. Pollard, T.D. Assays for myosin. *Methods Enzymol.* **85**, 123–130 (1982).
16. White, H.D. Special instrumentation and techniques for kinetic studies of contractile systems. *Methods Enzymol.* **85**, 698–708 (1982).
17. Chen, J. & Selvin, P.R. Thiol-reactive luminescent lanthanide chelates. *Bioconjugate Chem.* **10**, 311–315 (1999).
18. Selvin, P.R., Jancarik, J., Li, M. & Hung, L.-W. Crystal structure and spectroscopic characterization of a luminescent europium chelate. *Inorgan. Chem.* **35**, 700–705 (1996).
19. Xiao, M. *et al*. Conformational changes between the active-site and regulatory light chain of myosin as determined by luminescence resonance energy transfer: The effect of nucleotides and actin. *Proc. Natl. Acad. Sci. USA* **95**, 15309–15314 (1998).
20. Xiao, M. & Selvin, P.R. An improved instrument for measuring time-resolved lanthanide emission and resonance energy transfer. *Rev. Sci. Instrum.* **70**, 3877–3881 (1999).
21. Clegg, R.M., Murchie, A.I., Zechel, A. & Lilley, D.M. Observing the helical geometry of double-stranded DNA in solution by fluorescence resonance energy transfer. *Proc. Natl. Acad. Sci. USA* **90**, 2994–2998 (1993).
22. Vamosi, G., Gohlke, C. & Clegg, R. Fluorescence characteristics of 5-carboxytetramethylrhodamine linked covalently to the 5′ end of oligonucleotides: multiple conformers of single-stranded and double-stranded dye-DNA complexes. *Biophys. J.* **71**, 972–994 (1996).
23. Xiao, M. & Selvin, P.R. Quantum yields of luminescent lanthanide chelates and far-red dyes measured by resonance energy transfer. *J. Am. Chem. Soc.* **123**, 7067–7073 (2001).
24. Lakowicz, J.R. *Principles of Fluorescence* (Kluwer Academic, New York; 1999).